

ANALYSIS OF TRANSVERSE FIELD DISTRIBUTIONS IN PORRO PRISM RESONATORS

Igor A Litvin^{1,2}, Liesl Burger¹ and Andrew Forbes¹

¹CSIR National Laser Centre, PO Box 395, Pretoria 0001, South Africa

²B.I. Stepanov Institute of Physics of NAS of Belarus, F. Scaryna Av.,68, Minsk 220072, Belarus

ABSTRACT

A model to describe the transverse field distribution of the output beam from porro prism resonators is proposed. The model allows the prediction of the output transverse field distribution by assuming that the main areas of loss are located at the apexes of the porro prisms. Experimental work on a particular system showed some interesting correlations between the time domain behavior of the resonator and the transverse field output. These findings are presented and discussed.

Key words: porro prism resonator, petal (spot) transverse field distribution, second pulse

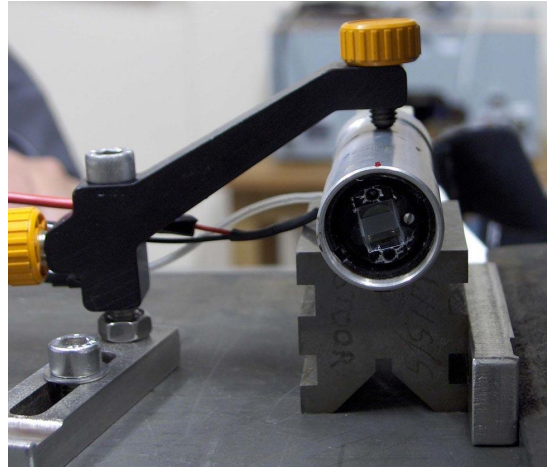
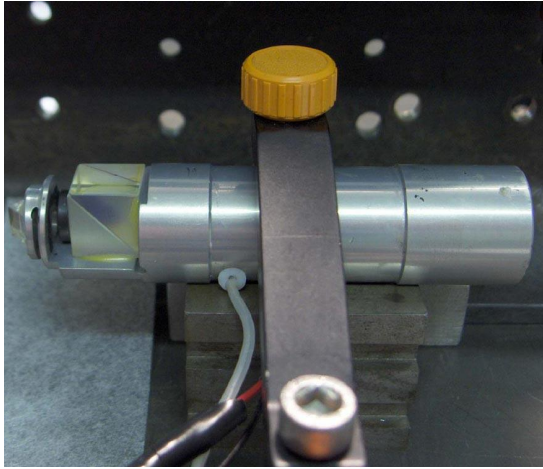
1. INTRODUCTION

Right angle prisms, often referred to as Porro prisms, have the useful property that all incident rays on the prism are reflected back parallel to the initial propagation direction, independent of the angle of incidence. Thus an initial planar wave front remains planar after reflection. This property was initially exploited in Michelson interferometers to relax the tolerances on mis-alignment, and then proposed in 1962 by Gould et al¹ as a means to overcome misalignment problems in optical resonators employing Fabry-Perot cavities, by replacing the end face mirrors with crossed roof prisms. Lasers based on this principle have been developed over the years²⁻⁶ with a review of the basic concepts and literature for Porro prisms specifically found in [7]. Much of the theoretical work to date has focused on geometric methods to model the inverting properties of such resonators²⁻⁴ and polarization considerations to account for internal phase shifts and output polarization states^{6,7}. In [2] the prism was modeled as a ray deviator by replacing an imaginary mirror some distance behind the prism. The model correctly accounted for the beam direction, but did not account for the complex field distribution found experimentally from the laser. Even the physical optics models fail to account for the true field pattern found from such resonators^{3,8}. In [3] for example, the kernel of the Fresnel-Kirchoff diffraction integral contains only the OPL experienced by the beam, thus treating the prism as though it were acting like a perfect mirror, with an identical ABCD matrix representation albeit incorporating the inverting properties of the prisms. This approach appears to be the preferred model for prisms⁷, even though it does not explain the complex transverse field patterns found in Porro prism resonators. This is a recurring problem in the literature, with only a hint at a solution offered in [8,9], where it is proposed to treat the field patterns as a result of diffractive coupling between a linear combination of sub-resonators. Anan'ev⁹, in considering the theoretical properties of resonators with corner cube prisms, specifically mentions the influence of bevels of finite width at the prism edges as a possible explanation for tendency for independent oscillation at different parts of the cross-section (looking down the length of the resonator), but does not go on to develop this idea into a model which can be used to explain experimental results.

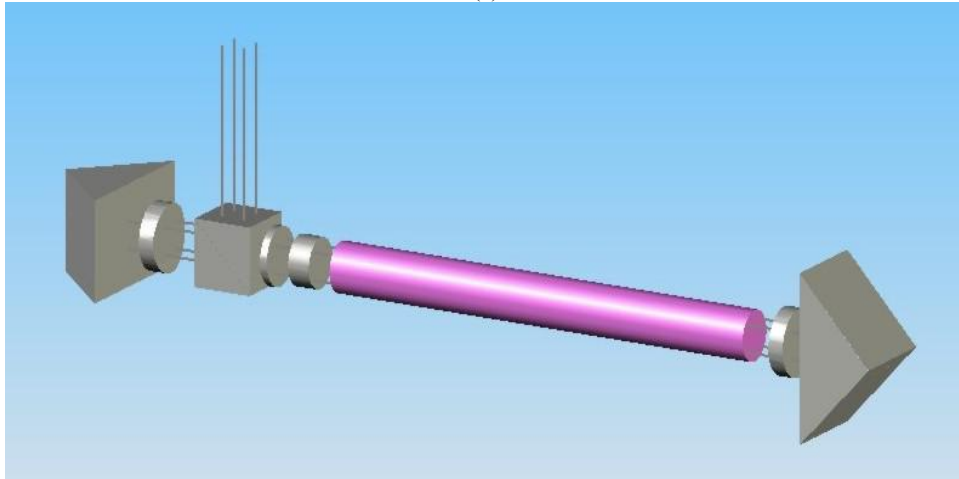
In this paper we have investigated the transverse field distribution of the output beam from a porro prism resonator (see fig.1). In section 2 we show experimental results on a resonator with two intra-cavity porro prisms. In section 3 we outline the necessary assumptions to build a model of this resonator, and generalize the results to provide a prediction of the behavior of such resonators at any angle between the prism apexes.

2. EXPERIMENT

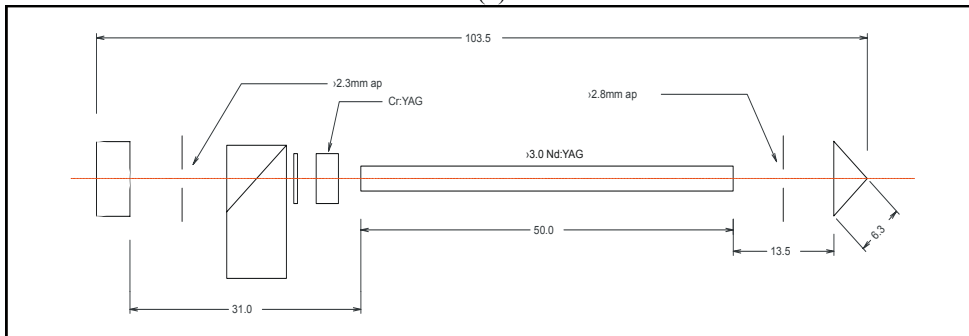
Petal field distribution. In this work we have investigated the spatial field distribution of the output beam of a porro prism resonator. The layout of the porro prism Nd:YAG laser with passive Q-switch laser which was used in our experiment is shown in Fig. 1. The porro prism resonator consisted of two porro prisms, with a quarter wave plate and polarization cube for the extraction of radiation from the cavity.



(a)



(b)



(c)

Fig. 1 (a-c): The porro prism Nd:YAG laser with passive Q-switch.

During experimental work some interesting properties of the spatial beam distribution in these types of cavities was observed, namely the dependence of the spatial field distribution on the angle between the porro prisms (ψ), defined to be the angle between the apexes of the porro prisms. For example, for crossed porro prisms this angle is $\psi = 90^\circ$. It was found that at some angles the field was arranged into a regular set of “petals” (see fig. 2a-b), while at other values of ψ a time varying field was observed (fig. 2c). In the case of the angles that generate the so called petal patterns, the number of petals, or spots, was found to depend on the angle ψ . Intensity profiles of the field distribution were obtained using an IR pyroelectric camera “spyricon”, and are shown in figure 2.

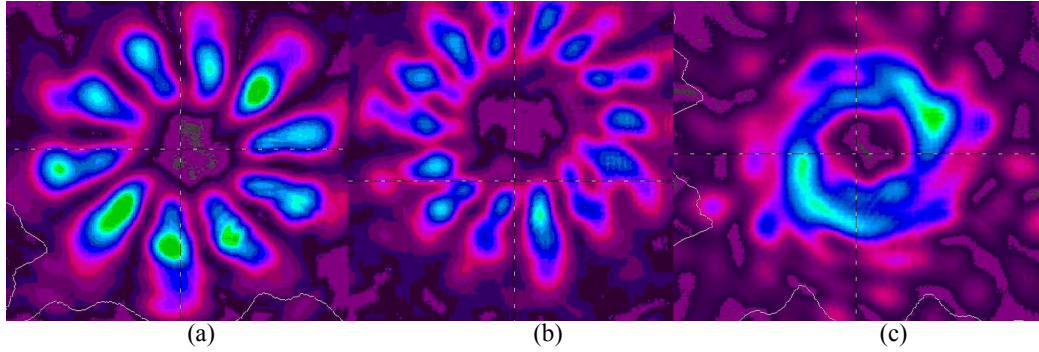


Fig. 2: Transverse field distribution of the output pulse of the Porro prism laser with the angles between Porro prisms (the relative error is half degree). (a) 72 degrees (b) 77 degrees (c) 79 degree (no spots).

It was found that a fixed set of angles existed at which the petal field distribution was observed. The experimental data of the angles (ψ) and the corresponding number of spots (N) are shown in Table 1.

| | | | | |
|-----------------|----|----|----|----|
| N | 16 | 10 | 14 | 18 |
| ψ , degree | 68 | 72 | 77 | 80 |

Table. 1: The experimental data of the angles between porro prisms and the number of spots corresponding to these angles.

The angles ψ for which an output beam existed for this laser were limited. In the given experiment the angles were between 63° and 87° . The absence of output below 63° was due to the increased misalignment between the porro prisms with decreasing angle away from 90° degrees (the crossed case). It should be noted that this is a particular artifact of the resonator under study, and is not a general property of such resonators. The absence of output above 87° degrees is due to the output coupling method of the given cavity. For example, at 90° (crossed prisms) the output beam does not exist because the losses are 100% due to complete output coupling from the cavity (ignoring phase shift under total reflection).

Second pulse. In some experiments it was found surreptitiously that when a second pulse was observed, so the spatial mode pattern from the resonator also changed. It was found that the observation of the second pulse was a function of the gain of the laser through the pump energy into the laser rod – below this threshold pumping no double pulse was observed, while above the threshold two pulses were consistently evident.

An interesting behavior of the transverse field distribution was observed for the second pulse. The transverse field distributions for the sum of the first and second pulses and also for first pulse are shown in Fig. 3.

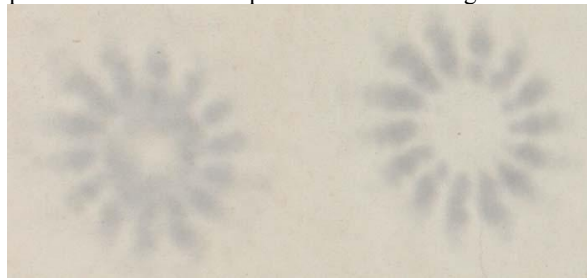


Fig.3: The transverse field distribution, with (a) two and (b) one pulse. The angle between the Porro prisms is 13 degrees (giving 14 spots).

It is apparent from Fig. 3 that the structure of the transverse field distribution of the second pulse differs from that of the first. This can be explained by the fact that in the region of the rod where first pulse was developed there are insufficient high-level electrons, and in the remaining regions there is a surplus. This is the reason for the development of the second pulse away from the region of the smallest losses.

3. RESONATOR MODEL

Having observed the generation of petal patterns inside the resonator at particular values of ψ , we wish to now develop a model that can explain why this happens, and can be used for predicting all the salient features of thus resonator.

3.1 Modeling the Porro prisms. For an understanding of the petal structure of the output beam the logical assumption will be used that the main losses from each of the two prisms take place on reflection from the apexes of the porro prisms.

Consider the field propagating back and forth along the resonator axis, and imagine viewing the resonator along its length from one prism looking towards the other. After reflecting off one prism, the field inverts itself around the prism edge, and reverses its propagation direction, traveling back towards the next prism. The same inversion and reversing of propagation direction takes place on each pass. Since losses are introduced onto the field from each prism, these losses also get inverted. The axis inversion (or reflection) depends on the angle between the two prisms. From the field inside resonator point of view, the equivalent picture is that of the field remaining inversion free, while the prisms themselves invert after each pass, essentially appearing to rotate, and hence the main area of loss (the apex edges) also appear to rotate. An example of this rotation is shown in Fig. 4.

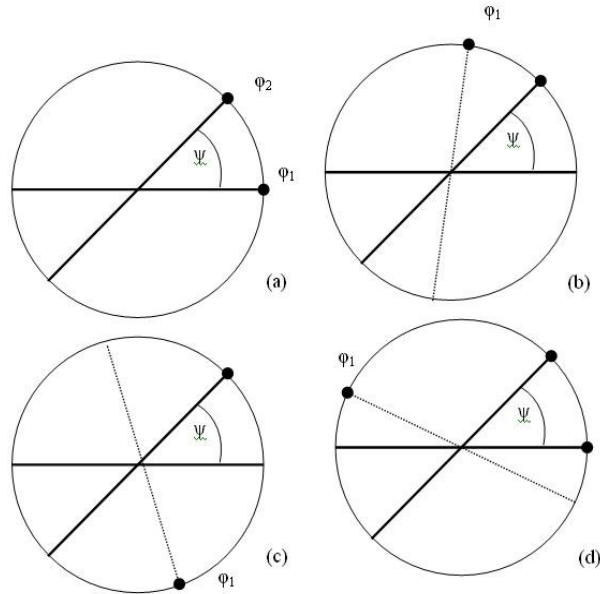


Fig. 4: (a)The roofs of two porro prisms . (b-d) The change in roof angle for both porro prisms after (b) 1 pass, (c) 2 passes, (d) 3 passes. (ϕ_1, ϕ_2 - angle of area of main loss of first and second roofs, ψ - angle between porro prisms.)

The prism rotation angles, and consequently the main areas of loss, are dependent on the number of passes, and can be found to be given by

$$\phi_1 = 2(-1)^n \psi \text{Floor}(0.9 + \frac{n}{2}), \quad (1a)$$

$$\phi_2 = 2(-1)^{n-1} \psi \text{Floor}(0.4 + \frac{n}{2}) + \psi, \quad (1b)$$

where n is the number of passes, ϕ_1, ϕ_2 are the new apparent angles of the loss areas of the first and second prisms respectively, and ψ is the angle between porro prisms inside the resonator.

A consequence of this model is that only at some discrete starting angles ψ will the rotating edges repeat on themselves, a necessary condition for a mode to be resonant inside the cavity. At these angles the field is sub-divided by the prisms losses, and it takes a certain number of passes for the subdivision of the field to be complete. At other angles the edges never repeat on themselves, thus infinitely sub-dividing the field. For example, for $\psi = 72^\circ$ we will have 10 sectors where we can expect pulse development; it follows that the petal field distribution will have 10 spots (see Fig. 2 and 6). Taking this into account, and considering the diffraction of a field propagating between areas of high losses it is reasonable to suppose that this is the explanation for the observed petal pattern at certain angles.

The equations (1a, b) can be used to calculate values of ψ for which the sub-division of the field is broken into a discrete and repeating. If the angles have a discrete set of values then we expect a spot pattern for this angle. But if the difference between neighboring angles of the discrete set is too small, then diffraction will blur the spot structure and no petal pattern will be observed. Figure 5 below shows angles at which the prisms edges find themselves as a function of the number of reflections (or passes).

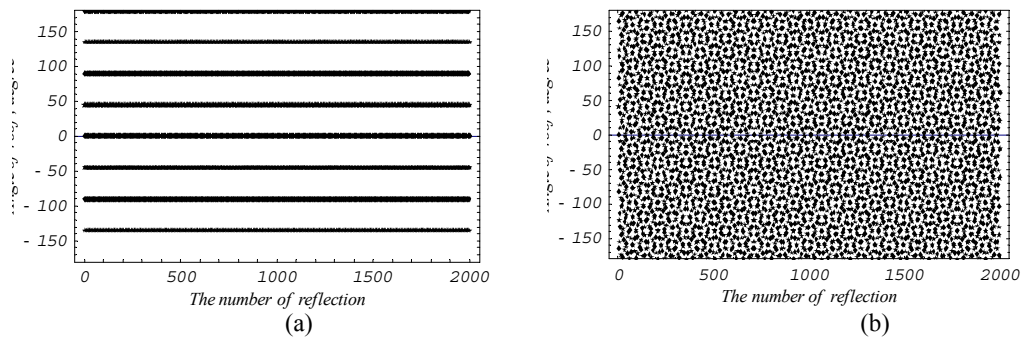


Fig. 5: The plots of the simulation of roof angles. The angles between porro prisms are (a) $\psi = 45^\circ$, (b) $\psi = 83^\circ$.

From Fig. 5 it is evident that for an angle between porro prisms of 45° the main area of loss has only a discrete set of angles, which repeat on themselves. In this case the beam inside the cavity will be strongly attenuated in this area and almost no attenuation in another. Therefore we expect that the spots will exist between these angles and in this case we have 8 equal intervals and 8 spots in the transverse distribution of the output beam. For the 83° case the areas of main loss have all possible values of angles, never seemingly to repeat, and so for this case we do not expect a field distribution comprising regular petals.

3.2 Numerical modeling. A numerical model of the rotation of main areas of losses for the porro prism resonator shown in Figure 1 was done using the software package GLAD. The output of the model is shown in Figure 6.

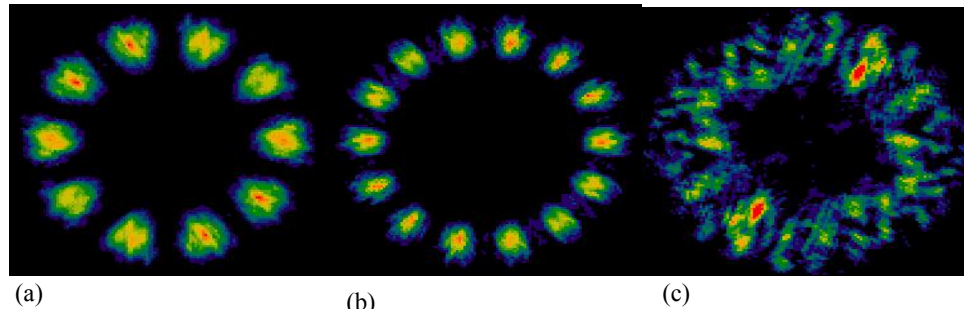


Figure 6: The transverse field distribution of the output pulse of a porro prism laser produced by the GLAD simulation. The angles between the porro prisms were (a) $\psi = 72^\circ$ (b) $\psi = 77^\circ$ (c) $\psi = 79^\circ$ (no spots).

This confirms the initial supposition that the main areas of loss are located at the apexes of the porro prisms, and spot field distribution of the output beam is in full agreement with this (see fig. 2, table 1 (experimental results) and fig.6, 7 (numerical simulation)).

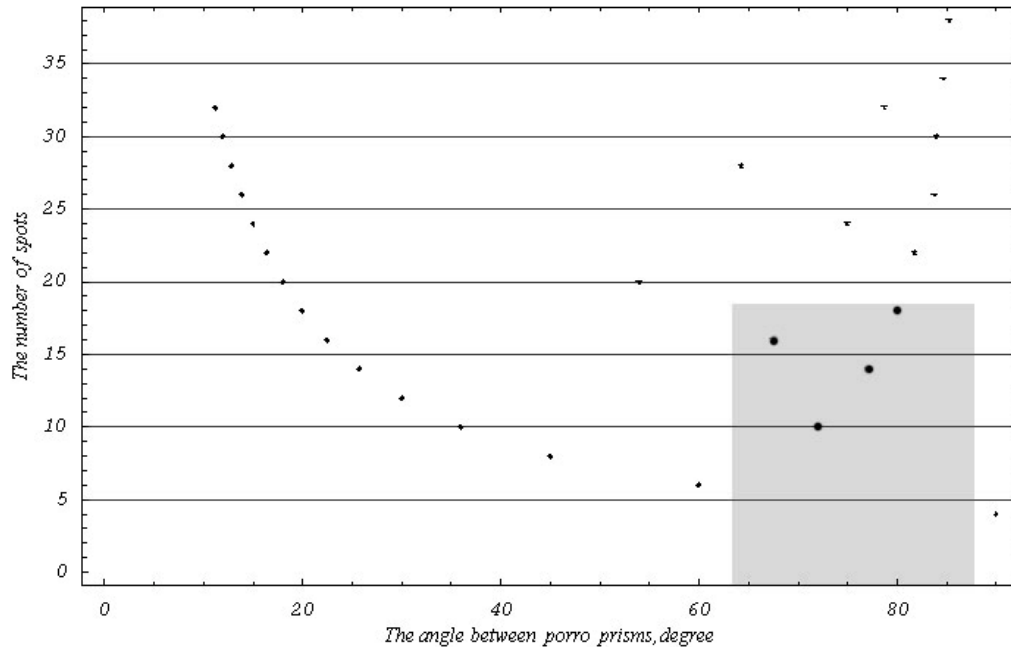


Fig. 7: The dependence of the number of spots on angle between porro prisms. The grey area is area where we could have output beam with spot distribution. The limitation of this area was discussed above. The bold points are points which we saw in experiment (see tab. 1).

4. CONCLUSIONS

In this work the transverse field distribution of the output beam of a porro prism laser was investigated both experimentally and numerically. It was found that for certain angles between the porro prisms this field had a petal like spot structure, which could be explain based on a model incorporating the apex losses of the prisms. It was also found that under certain conditions a second time pulse from the resonator was noted, with a modified transverse field structure. This can be explained by the fact that in the region of the rod where first pulse was developed there are insufficient high-level electrons, and in the remaining regions there is a surplus. This is the reason for the development of the second pulse away from the region of the smallest losses.

ACKNOWLEDGEMENTS

We would like to thank Denel Optronics for the use of their laser and for making experimental data available to us. We would also like to thank Dr Dieter Preussler and Mr Daniel Esser for useful discussions.

REFERENCES

1. G. Gould, S. Jacobs, P. Rabinowitz and T. Shultz., 1962. Crossed Roof Prism Interferometer, *Applied Optics* **1** (4), pp. 533 – 534.
2. I. Kuo and T. Ko., 1984. Laser resonators of a mirror and corner cube reflector: analysis by the imaging method, *Applied Optics* **23** (1), pp. 53 – 56.
3. G. Zhou and L.W. Casperson., 1981. Modes of a laser resonator with a retroreflecting roof mirror, *Applied Optics* **20** (20), pp. 3542 – 3546.
4. J. Lee and C. Leung., 1988. Beam pointing direction changes in a misaligned Porro prism resonator, *Applied Optics* **27** (13), pp. 2701 – 2707.
5. Y.A. Anan'ev, V.I. Kuprenyuk, V.V. Sergeev and V.E. Sherstobitov., 1977. Investigation of the properties of an unstable resonator using a dihedral corner reflector in a continuous-flow cw CO₂ laser, *Sov. J. Quantum Electron.*, **7** (7), pp. 822 – 824.
6. I. Singh, A. Kumar and O.P. Nijhawan., 1995. Design of a high-power Nd:YAG Q-switched laser cavity, *Applied Optics*, **34** (18), pp. 3349 – 3351.
7. N. Hodgson and H. Weber., 2005. *Laser Resonators and Beam Propagation* (2nd Ed.), Springer (New York), pp. 585 – 594.

8. Y.Z. Virnik, V.B. Gerasimov, A.L. Sivakov and Y.M. Treivish., 1987. Formation of fields in resonators with a composite mirror consisting of inverting elements, *Sov. J. Quantum Electron.*, **17** (8), pp. 1040 – 1043.
9. T.A. Anan'ev, 1973. Unstable prism resonators, **3** (1), pp. 58 – 59.